Nanofibrillar Patches of Commensal Skin Bacteria

Karine Glinel,[*,1,2] Adam Behrens,[2] Robert S. Langer,[2] Ana Jaklenec[2], Alain M. Jonas,*[*,1,2]

[1] Institute of Condensed Matter and Nanosciences, Université catholique de Louvain, Croix du Sud 1/L7.04.02, Louvain-la-Neuve, 1348, Belgium

[2] David H. Koch Institute for Integrative Cancer Research, Massachusetts Institute of Technology, 500 Main Street, Cambridge, MA 02139, USA

KEYWORDS. Layer-by-layer assembly; polymer nanotubes; commensal skin bacteria; *S. epidermidis*

ABSTRACT. We demonstrate entrapment of the commensal skin bacteria *Staphylococcus epidermidis* in mats composed of soft nanotubes made by membrane-templated layer-by-layer (LbL) assembly. When cultured in broth, the resulting nanofibrillar patches efficiently delay the escape of bacteria and their planktonic growth, while displaying high steady-state metabolic activity. Additionally, the material properties and metabolic activity can be further tuned by post-processing the patches with additional polysaccharide LbL layers. These patches offer a promising methodology for the fabrication of bacterial skin dressings for the treatment of skin dysbiosis while preventing adverse effects due to bacterial proliferation.

Introduction

The perturbation of the skin microbiota (or skin dysbiosis) is generally considered to be connected to a series of common skin pathologies.[1-3] Commensal skin bacteria occupy an important ecological niche in human beings,[4] and provide a range of beneficial effects to their hosts. This is especially true for *Staphylococcus epidermidis*, an ubiquitous gram-positive bacterium of the human skin that is known to limit *acne vulgaris*,[3] secrete antimicrobial substances such as phenol-soluble modulins,[5] stimulate the production of antibacterial peptides,[5] prevent nasal colonization by *Staphylococcus aureus* by secreting serine proteases,[6] counteract the influenza virus with extracellular matrix-binding proteins,[7] and modulate host immune response *via*, *e.g.*, staphylococcal lipoteichoic acids.[1,8] As a result, there is increasing interest in the use of *S. epidermidis* and other living skin bacteria as active components in skin-care products.[9] Problematically, *S. epidermidis* exists on the edge between pathogenicity and commensalism,[8,10] and has also been identified as a rapidly-evolving nosocomial pathogen.[11] Therefore, realizing the full clinical potential of *S. epidermidis* and other skin bacteria will require the development of methods that can maintain their beneficial effects while limiting the likelihood of adverse outcomes.

One such method would be to entrap living bacteria in a microporous soft material for direct application on skin. Specific hydrogels have been developed for the entrapment of living bacteria and the fabrication of 3D-printed skin tattoos.[12-14] Additionally, non-woven bacteria-containing gauzes have been produced for bioremediation and bioelectrochemistry, typically by microfluidics[15] and wet- or electro-spinning.[16-22] In such gauzes, the bacteria are usually directly entrapped in core-shell fibers, with a rigid hydrophobic porous shell surrounding a soft hydrogel

core containing the bacteria. In contrast, more fragile eukaryotic cells are generally seeded in mats of electrospun fibers after their fabrication, to preserve cell viability.[23-25]

Here, we explore an alternative route, based on the co-assembly of soft nanotubes and bacteria into hybrid patches. The selected nanotube production methodology is LbL assembly in the nanopores of a track-etched membrane, followed by membrane dissolution and nanotube recovery in aqueous suspension.[26-37] Nanofibrillar mats can be obtained by the simple sedimentation of LbL nanotubes on a filter.[38] Templated LbL assembly is especially interesting in the aim to incorporate a wide range of sensitive components in nanotubes, including enzymes and other biomacromolecules which do not always survive the harsher conditions of alternative techniques (*e.g.*, electrospinning). However, in the present article, we will limit ourselves to a proof-of-concept demonstration only involving nanotubes made from synthetic polyelectrolytes.

In this work, the bacterial patches are thus obtained by the forced sedimentation of mixed aqueous suspensions of LbL nanotubes and bacteria (Scheme 1). This procedure results in a highly porous structure that maintains bacterial metabolic activity while delaying bacteria escape and growth, thereby minimizing risks of bacteria proliferation and bacterial infection. We also demonstrate the ability to further tune material and metabolic characteristics of the patch through deposition of additional layers of polysaccharide polyelectrolytes. The resulting structures are well-suited for direct application or incorporation into gauzes and other skin dressings.

Materials and methods

Materials. Poly(styrene sulfonate) (PSS, average molar mass by weight 70 000 g/mol) and poly(allylamine hydrochloride) (PAH, average molar mass 450 000 g/mol) were purchased from Aldrich. They were dissolved (1 mg/mL) in 0.5 M NaCl/0.005 M $CaCl_2$/pH 7. Chitosan (CHI,

Protosan UP CL114 50 000-150 000 g/mol) was obtained from Novamatrix, and alginate (ALG, Ref-W201502, viscosity 5-40 cps at 1%, 25°C) was from Aldrich. They were dissolved (1 mg/mL) in 0.15 M NaCl/pH 6. NaCl (BioXtra, >99.5%), $CaCl_2$ (>93%) and dextran (from Leuconostoc spp., molar mass 40 000 g/mol) were from Aldrich. Track-etched membranes were kindly provided by it4ip (Belgium). The alamarBlue® cell viability reagent and the Live/Dead® BacLight™ Bacterial Viability Kit were obtained from Thermo-Fisher Scientific. All aqueous solutions were prepared using deionized water with a resistivity of 18.2 MΩ.cm at 25°C, and were sterilized in an autoclave prior to use.

Bacteria culture. Freeze-dried *S. epidermidis* from ATCC (ref. number 12228) was revived and cryo-preserved at -80°C as described previously.[39] When needed, the cryo-preserved bacteria were revived overnight in 5 mL of broth (BD Difco™ Nutrient Broth 234000) in 14 mL vented culture tubes (250 rpm, 37°C). The content of four such tubes was then poured into 700 mL broth in a vented culture flask, and grown at 37°C/250 rpm until reaching an optical density of ~0.55 (540 nm, cells of 1 cm path length). The bacteria were washed in 0.15 M NaCl at pH 6, concentrated by a factor of 20 by three successive steps of centrifugation/redispersion in NaCl 0.15 M at pH 6, and stored overnight in the fridge at 4°C. This concentrated bacteria suspension will be henceforth called *starting suspension*; it contains *ca*. 2.4×10^9 bacteria/mL (measured as detailed in the Supplementary Information).

Preparation of the LbL nanotubes. A 10x10 cm^2 untreated polycarbonate track-etched membrane (10^8 pores/cm^2, pore diameter 200 nm, thickness 25 μm) was used for nanotube fabrication. The membrane was alternately dipped for 10 min into a PSS and a PAH solution, with two intermediate rinsing steps of 30 s in 0.5 M NaCl/0.005 M $CaCl_2$/pH 7. Nine cycles of PSS/PAH adsorption were performed, starting by PSS. Each side of the membrane was decrusted

every third LbL cycle by scrubbing in pure water with a cotton pad; this rubbing step was successively performed in two orthogonal directions. The membrane was finally rinsed in pure water and dried on absorbing paper (Kim wipes).

The pore-filled membrane was then placed in 40 mL of dichloromethane (CH_2Cl_2) and gently shaken until fully dissolved. 4.2 g of dextran powder was then added to prevent the agglomeration of the released nanotubes upon filtration. The nanotube/dextran suspension was filtered onto a track-etched polyimide membrane (200 nm pore size) covered by *ca*. 300 mg of dextran powder to avoid adhesion of the nanotubes on the membrane. The collected nanotube/dextran powder was rinsed six times with 10 mL CH_2Cl_2 to eliminate traces of dissolved polycarbonate, then dried under vacuum in a sterile tube to remove any trace of solvent. Due to their passage in methylene chloride, the nanotubes are effectively sterile.

Preparation of the bacterial patches. The nanotube/dextran powder was added in sterile conditions with an aqueous solution (NaCl 0.15 M, pH 6, *qsp* 40 mL) to dissolve dextran and disperse the nanotubes. After gentle shaking (20 min), the suspension was transferred to four sterile tubes (10 mL suspension in each), and 10 mL of NaCl 0.15 M at pH 6 was added to the tubes. Considering the area (25 cm^2) and pore density (10^8 pores/cm^2) of the membrane used in the fabrication process, each tube thus contains *ca*. $2.5x10^9$ nanotubes in 20 mL aqueous solution. In one of these tubes, 0.293 mL of the starting bacteria suspension was added, corresponding to *ca*. $7x10^8$ bacteria.

The bacterial patches were prepared by successive filtration in sterile conditions of the nanotube suspensions over a track-etched polycarbonate membrane ($4x10^7$ pores/cm^2, 0.8 μm pore diameter, hydrophilic, 1.4 cm effective filtration diameter). The first layer was obtained by

filtration of 20 mL of nanotube suspension; the second layer was made from 20 mL of the bacteria-containing nanotube suspension; the third and final layer was made from 20 mL of the nanotube suspension. Each layer was rinsed with 5-10 mL of NaCl 0.15 M at pH 6 to eliminate traces of dextran; complete drying of the patches was avoided during the process. The bacterial patches were then stored upside down in NaCl 0.15 M, pH 6, at 4°C.

Post-coating of the bacterial patches. Chitosan/alginate multilayers were deposited on some bacterial patches by alternatively and cyclically dipping the patches for 5 min in chitosan then alginate solutions, with three intermediate rinses of 15 s in 0.15 M NaCl at pH 6, in sterile conditions in a biosafety cabinet.

Culture of the bacterial patches. Pieces of the patches (typically one fourth of a patch, corresponding to *ca*. 1.8×10^8 bacteria) were cultured in 8 mL broth (BD Difco™ Nutrient Broth 234000) in vented 14 mL culture tubes at 37°C, under constant orbital agitation (225 rpm). At specific time points, 0.25 mL of the supernatant was placed in a well of a 96 well plate and the optical density was measured at 540 nm with a Tecan plate reader. In order to cover a complete range of times, two such cultures were performed with a delay of 12 h, with partial overlap between the sampling times; the data of the two cultures were combined together to obtain the growth curve. The data were interpolated with a smoothing-spline routine, and the highest slope in the exponential growth phase was obtained by differentiation. The intercept of the line of highest slope with the zero-culture time base line was defined as the onset of growth. For these experiments, the negative control was pure broth; the positive control consisted of 0.073 mL of the starting bacterial suspension (*ca*. 1.8×10^8 bacteria) dispersed in 8 mL of broth; the starting amount of free bacteria was thus close to the one contained in the patches.

In parallel, smaller pieces of measured area (from 6 to 8.5 mm^2) of the same patch were placed in wells of a 96 well plate, containing 0.25 mL of broth and 25 μL of alamarBlue® cell viability reagent. The patches were placed vertically in the wells to avoid interfering with spectroscopic measurements, and the incubation was performed at 37°C. At specific time points, the fluorescence at 585 nm was measured under excitation at 570 nm (bandwidth of 5 nm) to evaluate the metabolic activity of the patches. Negative controls consisted of the pure broth, and of a patch without bacteria. The positive control was 0.00766 mL of the starting bacterial suspension in broth (*ca*. $1.8x10^7$ bacteria). The data was normalized by the area of the patches (or, for the positive control, by its equivalent area). The rate of metabolic activity was estimated as the slope of the fluorescence versus time, over the first 6h of culture.

Microscopy. Droplets of nanotube suspensions were observed with an optical Zeiss Axiovert 200 M microscope at 40x magnification. For confocal microscopy, the bacterial patches were stained for 20 min in the dark with a Live/Dead® BacLight™ mixture kit (SYTO® 9 (3.34 mM)/propidium iodide (20 mM) 50:50 v:v), and imaged with an Olympus FV1200 Laser Scanning Confocal Microscope (green channel, FITC). For scanning electron microscopy (SEM), the bacterial patches were first fixated by glutaraldehyde (2% in PBS) then dehydrated by successive immersion in alcohol/water mixtures (of increasing concentration in alcohol) and covered by 1.5-2 nm of gold (Cressington Sputter Coater 208HR) to reduce surface charge effects. The imaging was performed with a field emission scanning electron microscope (JSM-7600F, JEOL Ltd.), operated at 5 kV.

Results and discussion

Preparation and characterization of LbL nanotubes (Scheme 1). Soft LbL nanotubes were prepared by the cyclic adsorption of poly(styrene sulfonate) (PSS) and poly(allylamine hydrochloride) (PAH) within the pores of a polycarbonate track-etched membrane with pores of 200 nm diameter and 25 μm length, as described in previous publications.[30,34-36,38] In order to have a large increment of thickness per PSS/PAH bilayer, conditions of relatively high ionic strength were used during LbL deposition (0.5 M NaCl, 0.005 M $CaCl_2$, pH 7). Such conditions generate fully-filled nanopores after only a few cycles of adsorption,[38] leading to nanowires when the tube wall is swollen in water, and to nanotubes of *ca*. 60 nm tube wall thickness in the dry state (inset of Figure 1a). Here, nine cycles of adsorption were used to ensure full pore filling in water.

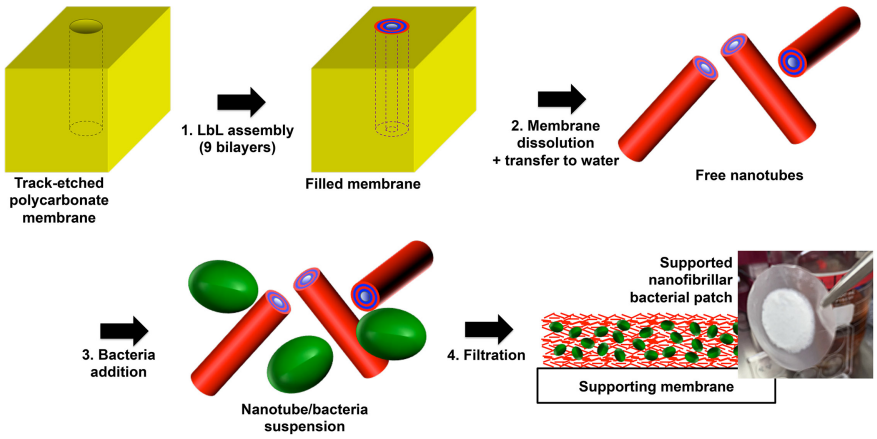

Scheme 1. Fabrication process of nanofibrillar bacterial patches based on LbL nanotubes. The picture at the bottom right shows a bacterial patch with an active region (white circle) of 1.4 cm diameter.

A suspension of $(PSS/PAH)_9$ nanotubes in organic solvent was then obtained by dissolving the membrane in CH_2Cl_2. Optical microscopy images indicated that straight nanotubes of expected

length are obtained at this stage (Figure 1a). The nanotubes were then transferred to 0.15 M NaCl aqueous solution at pH 6 according to a previously published protocol,[34-36,38] involving filtration in the presence of a CH_2Cl_2-insoluble but water-soluble powder (dextran). This process eliminates tube aggregation during collection. The nanotube shape was essentially preserved after the transfer process. However, due to the swelling of the polyelectrolyte nanotubes in water, a more tortuous morphology is seen (Figure 1b).

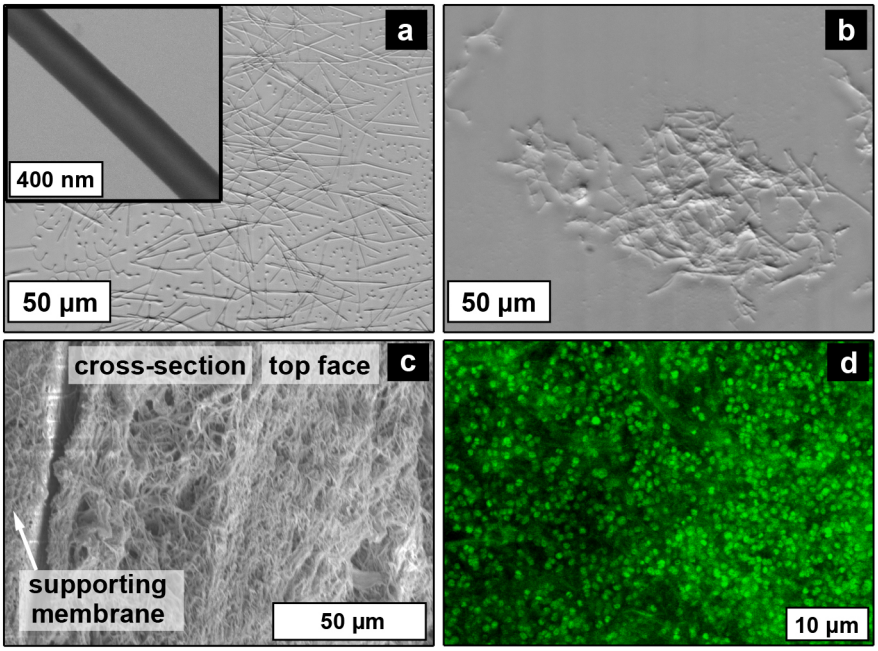

Figure 1. (a) Optical microscopy of the starting $(PSS/PAH)_9$ nanotubes (a) as collected after dissolution of the polycarbonate membrane in CH_2Cl_2. The inset is a SEM image of a single nanotube. (b) Optical microscopy of the $(PSS/PAH)_9$ nanotubes after their transfer to an aqueous solution. The diameters of the nanotubes in panels a and b are diffraction-limited. (c) SEM cross-section image of a bacterial patch over its supporting membrane. The bacteria are not visible due to the lack of electronic contrast. (d) Projected view of the green channel of confocal microscopy images of a bacterial patch, after Live/Dead® BacLight™ staining.

Preparation and microstructure of the bacterial patches. Mats of nanotubes were then prepared by forced sedimentation (filtration) of aqueous suspensions of nanotubes onto a porous polycarbonate membrane of 0.8 μm pore diameter which prevents the passage of both nanotubes and bacteria during the filtration process (Scheme 1). Three layers were successively sedimented, each of them containing *ca*. 2.5×10^9 tubes (based on the area of the templating membrane used to prepare the aqueous suspensions). To obtain bacteria-loaded patches, the second suspension used to fabricate the inner layer of the patch was added with *ca*. 0.7×10^9 *S. epidermidis* bacteria prior to sedimentation, of which *ca*. 80% are alive (as was measured before by Live/Dead® BacLight™ staining experiments)[39]. An image of a final membrane-supported bacterial patch is shown in Scheme 1: the total active diameter of the patch is typically 1.4 cm, and its bacterial content is *ca*. 4.6×10^8 bacteria/cm^2.

A small sample was cut in the bacterial patch; after drying and fixation by glutaraldehyde, it was imaged by scanning electron microscopy (SEM) (Figure 1c). Due to the limited electronic contrast between bacteria and nanotubes, it was not possible to directly observe the bacteria. However, the nanofibrillar and open texture of the patch is clearly observed, with a total patch thickness of *ca*. 55 μm. The SEM image also shows that the patch is composed of many small pores of diameter ranging between 0.5 and 1 μm, connected by a few bigger pores which can be as large as 10 μm. A complete analysis of the texture of bacteria-free mats of LbL nanotubes is available elsewhere.[38] Another section of the patch was then stained with the Live/Dead® BacLight™ mixture kit and imaged by confocal microscopy (Figure 1d and Supplementary Information movie S1), revealing a dense loading of bacteria. Because of strong light scattering, only the first top 10 μm of the sample could be imaged. Nevertheless, confocal microscopy

clearly showed that the bacteria were not restricted to the central layer of the patch, indicating that the successive filtration steps resulted in some blurring of the layers.

Bacterial activity. The bacterial activity was assessed in two ways. First, a piece of patch was cultured in broth in a shaken test tube, and the optical density of the supernatant broth was measured at regular time points. This experiment provides a direct measure of the escape of the bacteria from the patch and subsequent growth. In parallel, another sample of measured area (hence known number of bacteria) was cultured in broth in a 96-well plate, in the continuous presence of the alamarBlue® redox dye. The reduction by viable bacteria of the non-fluorescent resazurin blue dye into the red fluorescent resorufin dye provides a measure of the metabolic activity of the bacteria. Negative controls consisted of the pure broth and of a patch devoid of bacteria. The positive control was *ca*. 1.8×10^7 free bacteria in the broth, close to the number of entrapped bacteria ($2.8\text{-}3.9 \times 10^7$); to decrease variability, the free bacteria originated from the same culture as used to fabricate the patches.

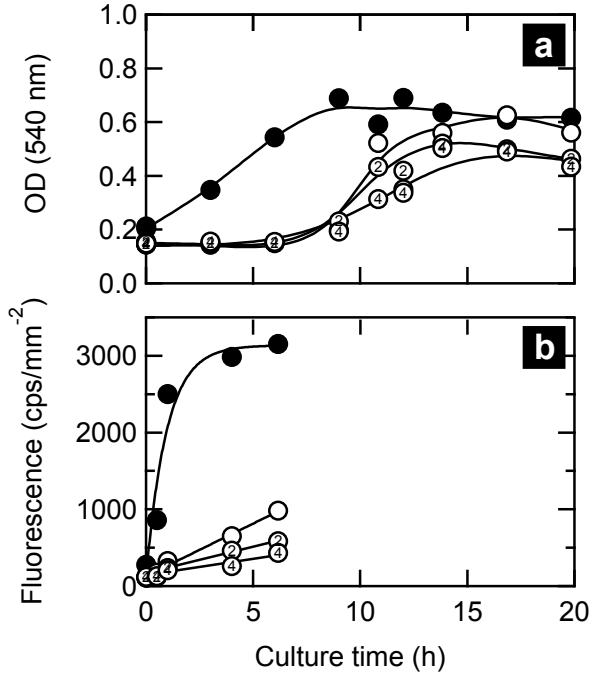

Figure 2. Optical density (a) and normalized metabolic activity (b) of the supernatant broth versus culture time at 37°C, in the presence of bacterial patches (open circles) or free bacteria (filled symbols). The numbers in the open symbols indicate the number of (chitosan/alginate) bilayers added onto the patch after fabrication. For the metabolic activity, the broth was added with 10 vol% alamarBlue®, and the fluorescence at 585 nm was measured; the data are normalized to the same starting number of bacteria by dividing by the patch area, or by an equivalent area for free bacteria.

Figure 2a shows the growth of escaped bacteria in the broth. Whereas the free bacteria grew directly with a half-time of *ca*. 4.5h, the growth of the bacteria trapped in the patch was delayed by *ca*. an additional 5.5h, with no growth visible for the first 6h. The metabolic activity is plotted versus culture time for the bacterial patch and the controls in Figure 3. The metabolic activity obtained from the fluorescence data was also normalized by the patch area or, for the positive control, by the equivalent area of a virtual patch containing 4.6×10^8 bacteria/cm^2 (Figure 2b).

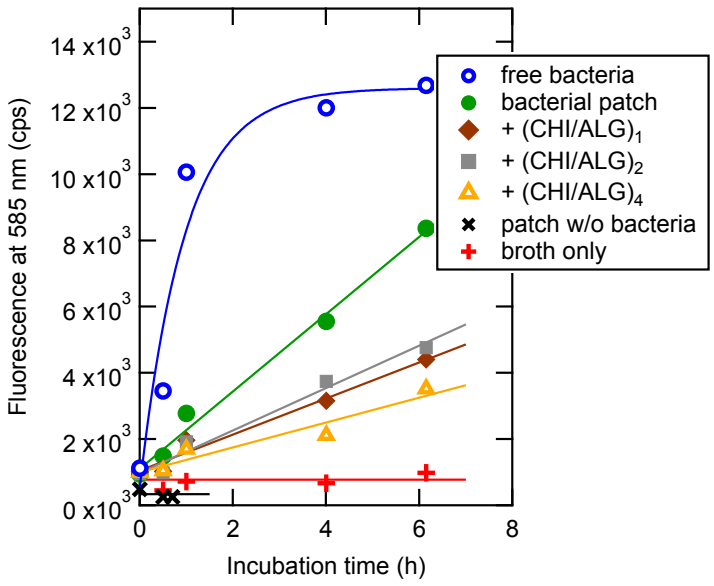

Figure 3. Fluorescence at 585 nm versus incubation time of bacterial patches cultured in broth with 10 vol% added alamarBlue® activity indicator. Some of the patches were coated by chitosan/alginate (CHI/ALG) multilayers as indicated in the caption. The area of the patches is 8.5, 6.2, 8.1 and 8.1 mm^2 for the uncoated patch and patches coated by one, two and four CHI/ALG bilayers, respectively, containing *ca*. $3.9x10^7$, $2.8x10^7$, $3.7x10^7$ and $3.7x10^7$ bacteria, respectively. The positive control consists of *ca*. $1.8x10^7$ free bacteria in broth; the negative controls are the broth (with 10 vol% alamarBlue®) or an uncoated patch without bacteria.

The negative controls showed no significant variation of fluorescence intensity over an incubation period of 6h, in contrast to the bacterial patch and the positive control. In contrast, the metabolic activity of the positive control increased strongly over the three first hours of culture then saturated, indicative of the exponential growth phase of the bacteria followed by the plateau regime. This is in agreement with the growth curves measured by optical density (Figure 2a). The bacterial patch also exhibited a significant linearly-increasing activity as soon as culture was started, indicating continuous metabolic activity of the bacteria trapped in the patch. Since no growth was detected in the supernatant broth over the six first hours, it can be concluded that the bacteria remain metabolically-active in the patches while initially not significantly growing in the broth.

Regulation of bacterial activity in the patches. To tune the bacterial activity of the patches, one can vary the amount of entrapped bacteria. However, it is also possible to add polyelectrolyte multilayers of increasing thickness to the patches, which should have the supplementary virtue to mechanically reinforce them. Based on our previous study of the coating of *S. epidermidis* by polyelectrolyte multilayers,[39] we selected chitosan (CHI) and alginate

(ALG) as polycation and polyanion, respectively. The coating of the membrane-supported bacterial patches was conveniently accomplished by their successive immersions in aqueous polyelectrolyte and rinsing solutions. The deposition process always started with a chitosan layer since both the bacteria and the nanotubes should have a negatively-charged outer surface, and always ended with an alginate layer. When coated by such alginate-ended $(CHI/ALG)_n$ shells, *S. epidermidis* was demonstrated to remain viable while exhibiting delayed growth due to the bacteriostatic effect of the polyelectrolyte multilayer.[39]

The growth of bacteria escaping from the patches is plotted in Figure 2a (symbols indicate the number of added (CHI/ALG) bilayers), while their surface-normalized and raw metabolic activity are shown in Figure 2b and 3, respectively. The onset of exponential growth (see Experimental section for a definition) is plotted in Figure 4a. The LbL coatings did not delay the growth of escaping bacteria as compared to the uncoated patches. We tentatively attribute this to the fact that some bacteria escaped from the sides of the cut patches which were not coated by the polyelectrolyte layers (indeed cutting was performed after the deposition of the polyelectrolyte layers). Additionally, since each bilayer only contributes *ca.* 2.2 nm to the coating thickness,[39] and the Young's modulus of water-equilibrated (ALG/CHI) coatings is reported to range from 4 to 20 MPa only,[40] the mechanical contribution of the LbL coating can only be marginal. Despite this, the metabolic activity over the first 6h of culture, a period of time during which the bacteria did not grow outside the patches, was significantly decreased by the addition of the (CHI/ALG) coatings (Figure 2b and 3). The rate of reduction of alamarBlue® per unit area of patch, averaged over the first 6h of culture, is presented in Figure 4b versus the number of added (CHI/ALG) bilayers. The activity decrease by a factor of *ca.* 3 observed upon

addition of four bilayers is attributed to the bacteriostatic effect of (CHI/ALG) coatings on bacteria, as we reported before.[39]

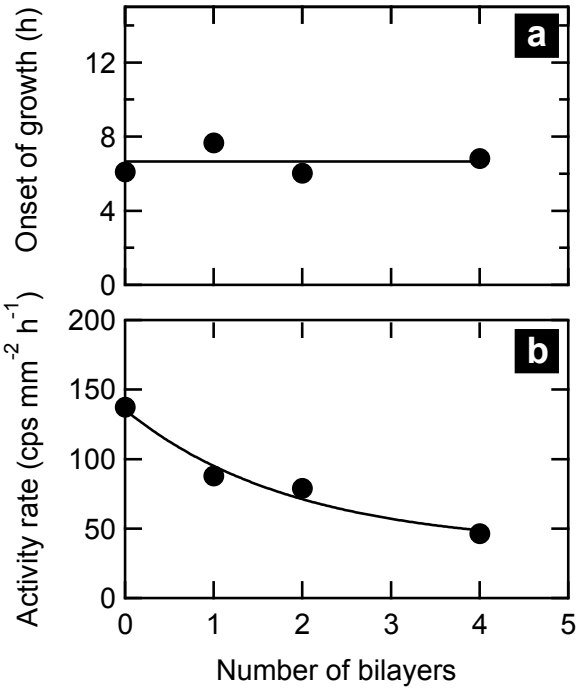

Figure 4. Onset of growth of bacteria having escaped from the bacterial patches into the supernatant broth (a) and average rate of reduction of the alamarBlue® dye by the bacteria trapped in the patches (b), versus the number of (CHI/ALG) bilayers added to the bacterial patches after fabrication.

The amount of escaped bacteria can be roughly estimated from the relationship between the concentration of free bacteria in the broth and the onset of bacterial growth, which we established in our previous work.[39] A delay of the growth by 6 h corresponds to *ca*. 2.4×10^5 bacteria/mL initial bacterial concentration in the broth,[39] hence *ca*. 1.9×10^6 bacteria in the 8 mL used here to test the growth of escaped bacteria. Compared to the *ca*. 1.8×10^8 bacteria in the tested pieces of patch, this corresponds to 1% of escaped bacteria. It should be emphasized that

the conditions we used to test bacterial escape in a strongly shaken broth are much more severe than the conditions typically met in topical applications. Therefore, much lower amounts of escaped bacteria are to be expected in more realistic cases.

It is also interesting to compare the rates of metabolic activity of free and entrapped bacteria, after normalization to the same amount of starting bacteria: the initial rate of reduction of alamarBlue® by free bacteria was larger by a factor of sixteen compared to the average rate measured for bacteria entrapped in a non-coated patch. This large difference arises from the free bacteria directly entering their exponential growth phase, in which bacteria multiply rapidly and have a strong metabolic activity. However, as Figure 2b shows, the free bacteria already entered their plateau phase after only three hours of culture. This is followed by a strong decrease in activity due to medium exhaustion and progressive cell death. In contrast, the entrapped bacteria had a more stationary behavior: A continuous and steady metabolic activity over six hours was observed. This demonstrates the benefit of having the bacteria trapped in such nanofibrillar patches, as it not only delays their escape and free growth, but also exhibits steady-state metabolic activity. This result has the potential to translate into a steady release of secreted molecules that are beneficial to the skin.

Conclusions

In summary, we have shown that the commensal bacteria *S. epidermidis* can be easily entrapped in patches of nanotubes made by membrane-templated layer-by-layer assembly. The resulting nanofibrillar patches effectively delay planktonic growth while keeping the bacteria metabolically-active. Interestingly, the trapped bacteria exhibit a steady metabolic activity over significantly longer culture times as compared to free bacteria. Additionally, this metabolic activity can be further tuned by post-coating the patches with supplementary LbL layers. These

patches are thus promising for the fabrication of bacterial skin dressings for the treatment of skin dysbiosis while preventing bacterial proliferation.

There are however a couple of improvements that need to be considered before turning to real-life applications, among which the improvement of the mechanical resistance of the patches in order to increase the entrapment time of the bacteria and fully prevent planktonic growth. In this respect, a precise evaluation of the number of escaped bacteria in topical skin application is yet to be performed. In addition, methods to prevent the blurring of the three-layered structure of the patch are to be devised; ways to do so are currently being explored. Once done, the simple methodology presented here would allow us to fabricate multi-bacterial patches wherein each bacterial type would be confined in its own layer. Meanwhile, artificial mixed bacterial communities can already be created by our methodology. Furthermore, the inclusion of bioactive compounds such as enzymes in the LbL nanotubes, as can be routinely done,[32,35,41,42] would provide access to artificial multifunctional bacterial patches of increased complexity. Considering the many possible variations of nanotube composition and size afforded by LbL, the nanofibrillar patches presented here are thus a significant step forward towards efficient bacterial skin dressings.

ASSOCIATED CONTENT

Supporting Information. The Supporting Information (Figure S1: bacteria counting experiments; Movie S1: 3D reconstruction of the green channel of a z-stack of confocal microscopy images of a non-coated bacterial patch) is available free of charge on the ACS Publications website at DOI:xxx.

AUTHOR INFORMATION

Corresponding Author

*e-mails: karine.glinel@uclouvain.be, alain.jonas@uclouvain.be

Author Contributions

The manuscript was written through contributions of all authors. All authors have given approval to the final version of the manuscript. *These authors contributed equally.

ACKNOWLEDGMENT

The authors thank Delphine Magnin (UCL) for SEM imaging, and Jeff Wyckoff (Swanson Biotechnology Center – Microscopy Core, MIT) and Lihong Jing (MIT) for CLSM imaging. Financial support was provided by the Fulbright Scholar Program (A.M.J.), the Louvain Fundation (A.M.J.), Wallonia-Brussels International (K.G.), and the FNRS (A.M.J. and K.G.). K.G. is Research Associate of the F. R. S.–FNRS.

REFERENCES

(1) Nakamizo, S.; Egawa, G.; Honda, T.; Nakajima, S.; Belkaid, Y.; Kabashima, K. Commensal Bacteria and Cutaneous Immunity. *Semin. Immunopathol.* **2014**, *37* (1), 73–80.

(2) Williams, M. R.; Gallo, R. L. The Role of the Skin Microbiome in Atopic Dermatitis. *Curr. Allergy Asthma Rep.* **2015**, *15* (11), 1–10.

(3) Xia, X.; Li, Z.; Liu, K.; Wu, Y.; Jiang, D.; Lai, Y. Staphylococcal LTA-Induced miR-143 Inhibits Propionibacterium Acnes-Mediated Inflammatory Response in Skin. *J. Invest. Dermatol.* **2016**, *136* (3), 621–630.

(4) Michael, T. M.; John, M. M.; Bender, K. S.; Buckley, D. H.; Stahl, D. A. *Brock Biology of Microorganisms*, 14 ed.; Pearson, 2015.

(5) Cogen, A. L.; Yamasaki, K.; Sanchez, K. M.; Dorschner, R. A.; Lai, Y.; MacLeod, D. T.; Torpey, J. W.; Otto, M.; Nizet, V.; Kim, J. E.; et al. Selective Antimicrobial Action Is Provided by Phenol-Soluble Modulins Derived From Staphylococcus Epidermidis, a Normal Resident of the Skin. *J. Invest. Dermatol.* **2010**, *130* (1), 192–200.

(6) Iwase, T.; Uehara, Y.; Shinji, H.; Tajima, A.; Seo, H.; Takada, K.; Agata, T.; Mizunoe, Y. Staphylococcus Epidermidis Esp Inhibits Staphylococcus Aureus Biofilm Formation and Nasal Colonization. *Nature* **2010**, *465* (7296), 346–349.

(7) Chen, H.-W.; Liu, P.-F.; Liu, Y.-T.; Kuo, S.; Zhang, X.-Q.; Schooley, R. T.; Rohde, H.; Gallo, R. L.; Huang, C.-M. Nasal Commensal Staphylococcus Epidermidis Counteracts Influenza Virus. *Sci. Rep.* **2016**, *6* (1), 1–12.

(8) Dong, Y.; Speer, C. P. The Role of Staphylococcus Epidermidis in Neonatal Sepsis: Guarding Angel or Pathogenic Devil? *Int. J. Med. Microbiol.* **2014**, *304* (5-6), 513–520.

(9) Reisch, M. S. The Microbiome Comes to Cosmetics. *Chem. Eng. News* **2017**, *95* (19), 30–34.

(10) Otto, M. Staphylococcus Epidermidis — the "Accidental" Pathogen. *Nat. Rev. Microbiol.* **2009**, *7* (8), 555–567.

(11) Schoenfelder, S. M. K.; Lange, C.; Eckart, M.; Hennig, S.; Kozytska, S.; Ziebuhr, W. Success Through Diversity - How Staphylococcus Epidermidis Establishes as a Nosocomial Pathogen. *Int. J. Med. Microbiol.* **2010**, *300* (6), 380–386.

(12) Schaffner, M.; Rühs, P. A.; Coulter, F.; Kilcher, S.; Studart, A. R. 3D Printing of Bacteria Into Functional Complex Materials. *Sci. Adv.* **2017**, *3* (12), eaao6804.

(13) Liu, X.; Yuk, H.; Lin, S.; Parada, G. A.; Tang, T.-C.; Tham, E.; la Fuente-Nunez, de, C.; Lu, T. K.; Zhao, X. 3D Printing of Living Responsive Materials and Devices. *Adv. Mater.* **2017**, *30* (4), 1704821.

(14) Liu, X.; Tang, T.-C.; Tham, E.; Yuk, H.; Lin, S.; Lu, T. K.; Zhao, X. Stretchable Living Materials and Devices with Hydrogel–Elastomer Hybrids Hosting Programmed Cells. *Proc. Natl. Acad. Sci.* **2017**, *114* (9), 2200–2205.

(15) Daniele, M. A.; North, S. H.; Naciri, J.; Howell, P. B.; Foulger, S. H.; Ligler, F. S.; Adams, A. A. Rapid and Continuous Hydrodynamically Controlled Fabrication of Biohybrid Microfibers. *Adv. Funct. Mater.* **2012**, *23* (6), 698–704.

(16) Klein, S.; Kuhn, J.; Avrahami, R.; Tarre, S.; Beliavski, M.; Green, M.; Zussman, E. Encapsulation of Bacterial Cells in Electrospun Microtubes. *Biomacromolecules* **2009**, *10* (7), 1751–1756.

(17) Gensheimer, M.; Brandis-Heep, A.; Agarwal, S.; Thauer, R. K.; Greiner, A. Polymer/Bacteria Composite Nanofiber Nonwovens by Electrospinning of Living Bacteria Protected by Hydrogel Microparticles. *Macromol. Biosci.* **2011**, *11* (3), 333–337.

(18) Klein, S.; Avrahami, R.; Zussman, E.; Beliavski, M.; Tarre, S.; Green, M. Encapsulation of Pseudomonas Sp. ADP Cells in Electrospun Microtubes for Atrazine Bioremediation. *J. Ind. Microbiol. Biotechnol.* **2012**, *39* (11), 1605–1613.

(19) Tong, H. W.; Mutlu, B. R.; Wackett, L. P.; Aksan, A. Manufacturing of Bioreactive Nanofibers for Bioremediation. *Biotechnol. Bioeng.* **2014**, *111* (8), 1483–1493.

(20) Knierim, C.; Enzeroth, M.; Kaiser, P.; Dams, C.; Nette, D.; Seubert, A.; Klingl, A.; Greenblatt, C. L.; Jérôme, V.; Agarwal, S.; et al. Living Composites of Bacteria and Polymers as Biomimetic Films for Metal Sequestration and Bioremediation. *Macromol. Biosci.* **2015**, *15* (8), 1052–1059.

(21) Kaiser, P.; Reich, S.; Leykam, D.; Willert-Porada, M.; Greiner, A.; Freitag, R. Electrogenic Single-Species Biocomposites as Anodes for Microbial Fuel Cells. *Macromol. Biosci.* **2017**, *17* (7), 1600442.

(22) Liu, Y.; Rafailovich, M. H.; Malal, R.; Cohn, D.; Chidambaram, D. Engineering of Bio-Hybrid Materials by Electrospinning Polymer-Microbe Fibers. *Proc. Natl. Acad. Sci.* **2009**, *106* (34), 14201–14206.

(23) Agarwal, S.; Wendorff, J. H.; Greiner, A. Use of Electrospinning Technique for Biomedical Applications. *Polymer* **2008**, *49* (26), 5603–5621.

(24) Tzezana, R.; Zussman, E.; Levenberg, S. A Layered Ultra-Porous Scaffold for Tissue Engineering, Created via a Hydrospinning Method. *Tissue Eng., Part C* **2008**, *14* (4), 281–288.

(25) Gorodzha, S. N.; Muslimov, A. R.; Syromotina, D. S.; Timin, A. S.; Tcvetkov, N. Y.; Lepik, K. V.; Petrova, A. V.; Surmeneva, M. A.; Gorin, D. A.; Sukhorukov, G. B.; et al. A Comparison Study Between Electrospun Polycaprolactone and Piezoelectric Poly(3-Hydroxybutyrate-Co-3-Hydroxyvalerate) Scaffolds for Bone Tissue Engineering. *Colloids Surf. B* **2017**, *160*, 48–59.

(26) Liang, Z.; Susha, A. S.; Yu, A.; Caruso, F. Nanotubes Prepared by Layer-by-Layer Coating of Porous Membrane Templates. *Adv. Mater.* **2003**, *15* (21), 1849–1853.

(27) Ai, S.; Lu, G.; He, Q.; Li, J. Highly Flexible Polyelectrolyte Nanotubes. *J. Am. Chem. Soc.* **2003**, *125* (37), 11140–11141.

(28) Tian, Y.; He, Q.; Cui, Y.; Li, J. Fabrication of Protein Nanotubes Based on Layer-by-Layer Assembly. *Biomacromolecules* **2006**, *7* (9), 2539–2542.

(29) Alem, H.; Blondeau, F.; Glinel, K.; Demoustier-Champagne, S.; Jonas, A. M. Layer-by-Layer Assembly of Polyelectrolytes in Nanopores. *Macromolecules* **2007**, *40* (9), 3366–3372.

(30) Roy, C. J.; Dupont-Gillain, C.; Demoustier-Champagne, S.; Jonas, A. M.; Landoulsi, J. Growth Mechanism of Confined Polyelectrolyte Multilayers in Nanoporous Templates. *Langmuir* **2010**, *26* (5), 3350–3355.

(31) Qu, X.; Komatsu, T. Molecular Capture in Protein Nanotubes. *ACS Nano* **2010**, *4* (1), 563–573.

(32) Komatsu, T.; Terada, H.; Kobayashi, N. Protein Nanotubes with an Enzyme Interior Surface. *Chem. Eur. J.* **2011**, *17* (6), 1849–1854.

(33) Komatsu, T. Protein-Based Nanotubes for Biomedical Applications. *Nanoscale* **2012**, *4* (6), 1910–1918.

(34) Saghazadeh, S.; Zhang, S.; Lefèvre, D.; Le Beulze, A.; Jonas, A.; Demoustier-Champagne, S. A Universal Method to Transfer Membrane Templated Nano-Objects to Aqueous Solutions. *Langmuir* **2015**, *31* (26), 7264–7273.

(35) Zhang, S.; Demoustier-Champagne, S.; Jonas, A. Quantitative Collection and Enzymatic Activity of Glucose Oxidase Nanotubes Fabricated by Templated Layer-by-Layer Assembly. *Biomacromolecules* **2015**, *16* (8), 2382–2393.

(36) Ramírez-Wong, D. G.; Saghazadeh, S.; Van Herck, S.; De Geest, B. G.; Jonas, A. M.; Demoustier-Champagne, S. Uptake of Long Protein-Polyelectrolyte Nanotubes by Dendritic Cells. *Biomacromolecules* **2017**, *18* (12), 4299–4306.

(37) Ramirez-Wong, D. G.; Bonhomme, C.; Demoustier-Champagne, S.; Jonas, A. M. Layer-by-Layer Assembly of Brushes of Vertically-Standing Enzymatic Nanotubes. *J. Coll. Interf. Sci.* **2018**, *514*, 592–598.

(38) Zhang, S.; Vlémincq, C.; Wong, D. R.; Magnin, D.; Glinel, K.; Demoustier-Champagne, S.; Jonas, A. M. Nanopapers of Layer-by-Layer Nanotubes. *J. Mater. Chem. B* **2016**, *4* (47), 7651–7661.

(39) Jonas, A. M.; Glinel, K.; Behrens, A.; Anselmo, A. C.; Langer, R. S.; Jaklenec, A. Controlling the Growth of Staphylococcus Epidermidis by Layer-by- Layer Encapsulation. *ACS Appl. Mater. Interf.* **2018**, *10* (19), 16250–16259.

(40) Silva, J. M.; Caridade, S. G.; Costa, R. R.; Alves, N. M.; Groth, T.; Picart, C.; Reis, R. L.; Mano, J. F. pH-Responsiveness of Multilayered Films and Membranes Made of Polysaccharides. *Langmuir* **2015**, *31* (41), 11318–11328.

(41) Hou, S.; Wang, J.; Martin, C. R. Template-Synthesized Protein Nanotubes. *Nano Lett.* **2005**, *5* (2), 231–234.

(42) Komatsu, T.; Sato, T.; Boettcher, C. Human Serum Albumin Nanotubes with Esterase Activity. *Chem. Asian J.* **2011**, *7* (1), 201–206.

TOC GRAPHICS